Synthesis of Mesoporous BN and BCN Exhibiting Large Surface Areas via Templating Methods

Ajayan Vinu,*,† Mauricio Terrones,†,‡ Dmitri Golberg,§,|| Shunichi Hishita,§ Katsuhiko Ariga,§ and Toshiyuki Mori§

International Center for Young Scientists, National Institute for Materials Science, 1-1 Namiki, Tsukuba, Ibaraki 305-0044, Japan, Advanced Materials Department, IPICyT, Camino a la Presa San José 2055, Lomas 4a sección, San Luis Potosí 78216, México, Advanced Materials Laboratory, National Institute for Materials Science, 1-1 Namiki, Tsukuba, Ibaraki 305-0044, Japan, and Nanomaterials Laboratory, National Institute for Materials Science, 1-1 Namiki, Tsukuba, Ibaraki 305-0044, Japan

Received August 9, 2005
Revised Manuscript Received October 10, 2005

Introduction

Porous materials such as activated carbons, zeolites, silica gels, and inorganic oxides are of great interest because of their potential applications in adsorption, catalysis, separation, purification processes, optics, electronics, etc.[1−6] In recent years there has been growing interest in the development of mesoporous materials with tailored pore structures.[7−19] Among these materials, mesoporous carbons have attracted considerable attention because of their remarkable properties, such as high specific surface areas, large specific pore volumes, chemical inertness, and good chemical and mechanical stability.[13−19] Mesoporous carbons can be easily prepared by template methods where mesoporous metal oxides are used as templates. They have also been used as templates for the synthesis of various mesoporous oxides such as MgO, Al_2O_3, and TiO_2.[20,21]

Hexagonal boron nitride (BN), which structurally resembles graphite, is an insulator exhibiting a band gap of ca. 5.5 eV, chemically inert, and thermally stable up to 1600 °C.[22,23] It is an excellent candidate for high temperature and protective coating applications.[22−24] It has also been found that partial substitution of BN by carbon would alter its hardness and electronic properties.[23] Due to these particular characteristics, many efforts have been focused on the preparation and application of BN and BCN (boron carbon nitride) nanomaterials.[25−32] BN and BCN nanotubes can be easily prepared via substitution reaction utilizing carbon nanotubes as templates.[25−32] By constructing BN and BCN structures, exhibiting ordered arrays of channels, novel applications could emerge: from catalysis, to molecular separations and sorption of very bulky molecules, and to the fabrication of semiconductors, semiconducting nanowires, and low dielectric devices. Recently, Han et al. have reported the preparation of disordered porous activated BN using activated carbon as a template.[33] However, this material displays very low specific surface area and pore volume. Very recently, Vinu et al. have successfully reported the preparation of well-ordered mesoporous carbon nitride materials using mesoporous silica as a template.[34] However, there has been no reports on the preparation of BN and BCN using the subsititution reaction method. In the present communication, we report for the first time the preparation of mesoporous boron nitride (MBN) and mesoporous carbon nitride (MBCN) with a very high surface area and pore volume. The materials were fabricated via substitution reactions at high temperatures (1500 to 1750 °C), using a well-ordered hexagonal mesoporous carbon as a template and boron trioxide as a boron source. The mesoporous carbon materials were prepared using mesoporous silica as a

* To whom correspondence should be addressed. Phone: +81-29-851-3354 (ext 8679). Fax: +81-29-860-4706. E-mail: vinu.ajayan@nims.go.jp.
† National Institute for Materials Science.
‡ IPICyT.
§ Advanced Materials Laboratory, National Institute for Materials Science.
|| Nanomaterials Laboratory, National Institute for Materials Science.

(1) Wu, C.; Bein, T. *Science* **1994**, *266*, 1013.
(2) Zakhidov, A. A.; Baughman, R. H.; Iqbal, Z.; Cui, C.; Khayrullin, I.; Dantas, S. O.; Marti, J.; Ralchenko, V. G. *Science* **1998**, *282*, 897.
(3) Mann, S.; Ozin, G. A. *Nature* **1996**, *382*, 313.
(4) Sun, J.; Shan, Z.; Maschmeyer, T.; Moulijn, J. A.; Coppens, M. O. *Chem. Commun.* **2001**, 2670.
(5) Subramoney, S. *Adv. Mater.* **1998**, *10*, 1157.
(6) Fan, S.; Chapline, M. G.; Franklin, N. R.; Tombler, T. W.; Cassel, A. M.; Dai, H. *Science* **1999**, *283*, 512.
(7) Kresge, C. T.; Leonowicz, M. E.; Roth, W. J.; Vartuli, J. C.; Beck, J. S. *Nature* **1992**, *359*, 710.
(8) Vinu, A.; Murugesan, V.; Hartmann, M. *Chem. Mater.* **2003**, *15*, 1385.
(9) Hartmann, M.; Vinu, A. *Langmuir* **2002**, *18*, 8010.
(10) Vinu, A.; Murugesan, V.; Böhlmann, W.; Hartmann, M. *J. Phys. Chem. B* **2004**, *108*, 11496.
(11) Vinu, A.; Murugesan, V.; Hartmann, M. *J. Phys. Chem. B* **2004**, *108*, 7323.
(12) Vinu, A.; Murugesan, V.; Tangermann, O.; Hartmann, M. *Chem. Mater.* **2004**, *16*, 3056.
(13) Ryoo, R.; Joo, S. H.; Jun, S.; *J. Phys. Chem. B* **1999**, *103*, 7743.
(14) Han, S.; Kim, S.; Lim, H.; Choi, W.; Park, H.; Yoon, J.; Hyeon, T. *Microporous Mesoporous Mater.* **2003**, *58*, 131.
(15) Yoon, S. B.; Kim, J. Y.; Yu, J. S. *Chem. Commun.* **2002**, 1536.
(16) Vinu, A.; Streb, C.; Murugesan, V.; Hartmann, M. *J. Phys. Chem. B* **2003**, *107*, 8297.
(17) Vinu, A.; Ariga, K. *Chem. Lett.* **2005**, *34*, 674.
(18) Vinu, A.; Miyahara, M.; Ariga, K. *J. Phys. Chem. B* **2005**, *109*, 6436.
(19) Vinu, A.; Hartmann, M. *Catal. Today* **2005**, *102*, 189.
(20) Roggenbuck, J.; Tiemann, M. *J. Am. Chem. Soc.* **2005**, *127*, 1096.
(21) Dong, A.; Ren, N.; Tang, Y.; Wang, Y.; Zhang, Y.; Hua, W.; Gao, Z. *J. Am. Chem. Soc.* **2003**, *125*, 4976.
(22) Loiseau, A.; Willaime, F.; Demoncy, N.; Schramchenko, N.; Hug, G.; Colliex, C.; Pascard, H. *Carbon* **1998**, *36*, 743.
(23) Pattanayak, J.; Kar, T.; Scheiner, S. *J. Phys. Chem. A 2002*, *106*, 2970.
(24) Palen, E. B.; Rummeli, M. H.; Knupfer, M.; Behr, G.; Biedermann, K.; Gemming, T.; Kalenczuk, R. J.; Pichler, T. *Carbon* **2005**, *43*, 615.
(25) Golberg, D.; Bando, Y.; Kurashima, K.; Sato, T. *Carbon* **2000**, *38*, 2017.
(26) Wu, J.; Han, W. Q.; Walukiewicz, W.; Ager, J. W.; Shan, W.; Haller, E. E.; Zettl, A. *Nano Lett.* **2004**, *4*, 647.
(27) Ma, R.; Bando, Y.; Sato, T.; Golberg, D.; Zhu, H.; Xu, C.; Wu, D. *Appl. Phys. Lett.* **2002**, *27*, 5225.
(28) Terrones, M.; Hsu, W. K.; Terrones, H.; Zhang, J. P.; Ramos, S.; Hare, J. P.; Castilo, R.; Prassides, K.; Cheetham, A. K.; Kroto, H. W.; Walton, D. R. M. *Chem. Phys. Lett.* **1996**, *259*, 568.
(29) Han, W. Q.; Bando, Y.; Kurashima, K.; Sato, T. *Jpn. J. Appl. Phys.* **1999**, *38*, L755.
(30) Golberg, D.; Bando, Y.; Han, W. Q.; Kurashima, K.; Sato, T. *Chem. Phys. Lett.* **1999**, *308*, 337.
(31) Han, W. Q.; Bando, Y.; Kurashima, K.; Sato, T. *Appl. Phys. Lett.* **1998**, *73*, 3085.
(32) Han, W. Q.; Mickelson, W.; Cuming, J.; Zettl, A. *Appl. Phys. Lett.* **2002**, *81*, 1110.
(33) Han, W. Q.; Brutchey, R.; Tilley, T. D.; Zettl, A. *Nano Lett.* **2004**, *4*, 173.
(34) Vinu, A.; Ariga, K.; Mori, T.; Nakanischi, T.; Hishita, S.; Golberg, D.; Bando, Y. *Adv. Mater.* **2005**, *17*, 1648.

10.1021/cm051780j CCC: $30.25
Published on Web 11/01/2005

template and sucrose as a carbon source.[13,16] We found that the specific surface area, specific pore volume, and pore diameter of the MBN and MBCN materials are much higher when compared to those observed in activated BN and BCN materials.[33]

Experimental Section

The method for the preparation of MBN is as follows: 20 mg of mesoporous carbon template was heated together with 400 mg of B_2O_3 in a flow of nitrogen (inlet flow 3 L/min and outlet flow 2 L/min) at 1750 °C for 45 min. The mesoporous carbon template was placed above a cleaned graphitic crucible containing B_2O_3. The heating was carried out in a vertical induction furnace. The reaction temperature was monitored using an optical pyrometer with the accuracy of ±10 °C. The MBCN with different carbon contents were prepared by heating 20 mg of mesoporous carbon with 200 mg of B_2O_3 in a flowing nitrogen at 1450−1550 °C for 30 min. These samples were labeled MBCN(*X*) where *X* denotes the reaction temperature. The MBN and MBCN were analyzed using JEOL-3000F and JEOL-3100FEF field emission high-resolution transmission electron microscopes equipped with a Gatan-766 electron energy-loss spectrometer (EELS) and an in-column Omega Filter, respectively. The EELS line-scan technique was employed in addition to the standard EELS mode. The samples were prepared by crushing the as-synthesized flakes in an agate mortar, mixing them with ethanol, sonication, and spreading the resultant mixture on a holey carbon film supported on a Cu grid. The textural parameters of the samples were obtained by nitrogen adsorption−desorption isotherms measured at −196 °C on a Quantachrome Autosorb 1 sorption analyzer. All samples were outgassed for 3 h at 250 °C under vacuum ($p < 10^{-5}$ hPa) in the degas port of the adsorption analyzer. The specific surface area was calculated using the BET model. The pore size distributions were obtained from the adsorption branch of isotherm using the corrected form of the Kelvin equation by means of the Barrett−Joyner−Halenda method.

Results and Discussion

Figure 1a−f shows HRTEM images of the mesoporous carbon, MBCN, and MBN materials. The inset shows the corresponding diffraction pattern (DP) of the ordered channels. The MBCN materials exhibit (Figure 1b−c) well-ordered mesoporous structure identical to the mesoporous carbon template, while MBN (Figure 1d) shows a less ordered mesoporous structure. Higher magnification of the image of the MBCN material (shown in Figure 1e) clearly displays the well-ordered mesoporous BCN layers with local interlinking of crystalline BCN layers. This indicates that the mesoporous carbon walls, which were previously amorphous, are completely transformed into the crystalline BCN walls during the substitution reaction. However, the magnified image of MBN (Figure 1f) shows a disordered BN framework with highly crystalline layers of BN. Elemental mapping studies of MBCN (Figure 2b−d) constructed using a standard three-window procedure (slit width 20 eV) reveal that the material is indeed composed of B (Figure 2b), C (Figure 2c), and N (Figure 2d). The traces of other elements were not detected using this technique. It can also be seen from the elemental mappings that the B, C, and N species are homogeneously distributed in all parts of the sample.

The elemental composition and the structure of MBN and MBCN were analyzed by EEL spectroscopy. The EEL

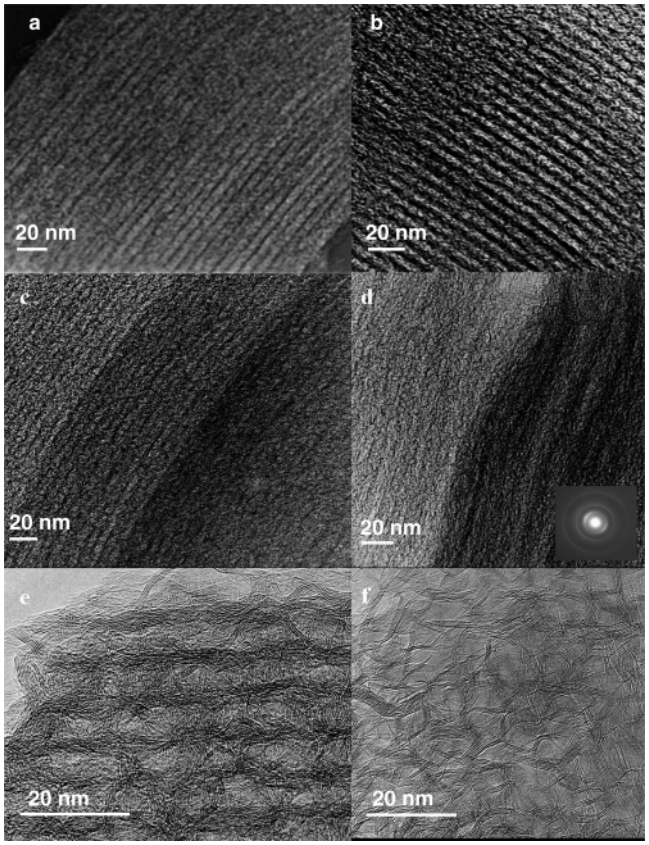

Figure 1. HRTEM images of mesoporous (a) carbon, (b) MBCN(1450), (c) MBCN(1550), and (d) MBN; (e) high magnification image of MBCN-(1550); and (f) high magnification image of MBN. Inset shows the corresponding diffraction pattern.

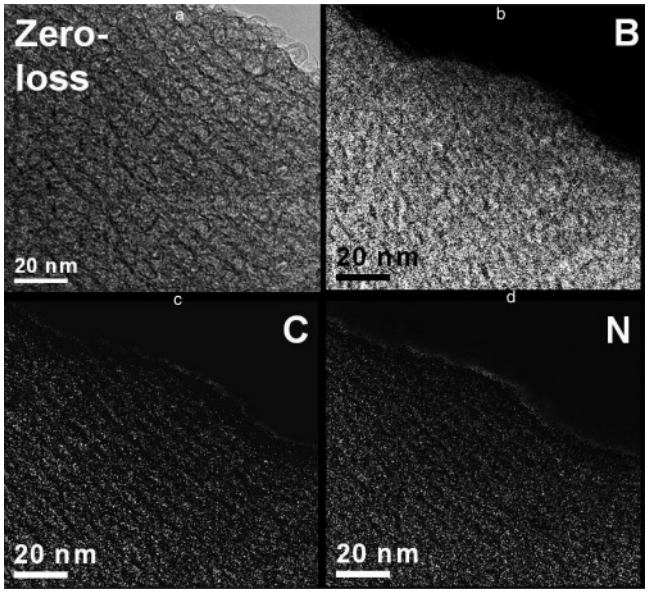

Figure 2. (a) HRTEM image of MBCN(1450). (b−d) Elemental maps of B, C, and N, respectively.

spectra of MBCN (Figure 3) clearly show the presence of the K-shell excitation shells of carbon, boron, and nitrogen, while the spectrum for MBN depicts only the presence of K edges corresponding to B and N. Sharp π^*-peaks (left-hand sides of the B and N K-shell excitation edges) and the shape of σ^*-bands (right-hand sides of the edges) are characteristics of the sp^2-bonding character of B and N atoms of the layers. The boron-to-nitrogen ratio calculated from the EEL spec-

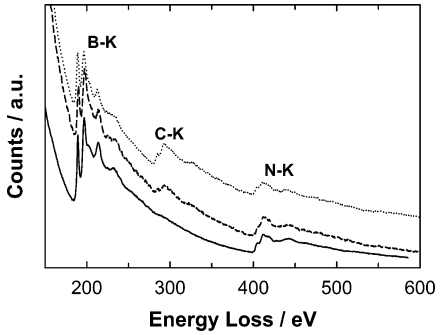

Figure 3. EEL spectra of mesoporous BN and BCN materials: (···) MBCN(1450), (- - -) MBCN(1550), and (—) MBN.

trum corresponding to MBN is 1.0 ± 0.05, which is in good agreement with the BN stoichiometry. The absence of the carbon signal in the MBN sample could be attributed to the high reaction temperature and the oxidation atmosphere used in the process. EELS analyses also show a variation of the carbon content as a function of synthesis temperature.

Figure 3 also displays the EELS spectrum of MBCN(1450) and MBCN(1550) samples prepared at different synthesis temperatures. It can be clearly seen from the figure that the intensity of C K-shell excitation edges increases as the reaction temperature is lowered. In particular, we observed that as the synthesis temperature decreases to 1550 and 1450 °C, an increase of the carbon content was observed (8.0 and 20.1 at. % for 1550 and 1450 °C respectively). From Figure 3, it is also possible to note that both MBCN samples reveal the characteristic B and C ionization edges corresponding to a graphite-like sp^2-bonded network with B/C ratio ranging from 0.08 to 0.2. The fine structure of the edges is mainly attributed to the 1s-π^* electron transition.

Elementary composition of MBN and MBCN samples were also analyzed by XPS technique. The XPS survey spectrum of MBN shows sharp signals for B and N and does not show any peaks for other elements except O (Figure 1S, see Supporting Information). It is a well-known fact that XPS is very sensitive toward O and the signal for O mainly comes from the moisture, ethanol, or atmospheric O_2 adsorbed on the surface of MBN. The overall boron-to-nitrogen ratio of MBN obtained from the XPS analysis is 0.94, which is very close the value obtained from the EELS. The XPS survey spectrum of MBCN(1450) shows four sharp signals for B, N, C, and O (Figure 2S, Supporting Information). The following elemental composition was obtained for the MBCN(1450) sample: $B_{21.1}C_{37.7}N_{23.0}O_{18.2}$.

The morphology of the mesoporous carbon, MBN and MBCN(1550) was also studied using a high-resolution scanning electron microscope (SEM). Figure 4 displays the SEM images of the original mesoporous carbon, as well as the MBN and MBCN(1550) materials. The appearance of the MBN and MBCN(1550) is almost similar to that of the mesoporous carbon; not only due to the fact that all of them exhibit monodispersed rod-like morphology but also in their length and diameter. This surprising similarity in the surface morphology of all samples confirmed that the surface morphology of the mesoporous carbon is retained in the MBN and MBCN samples, even when the synthesis temperature occurred above 1750 °C.

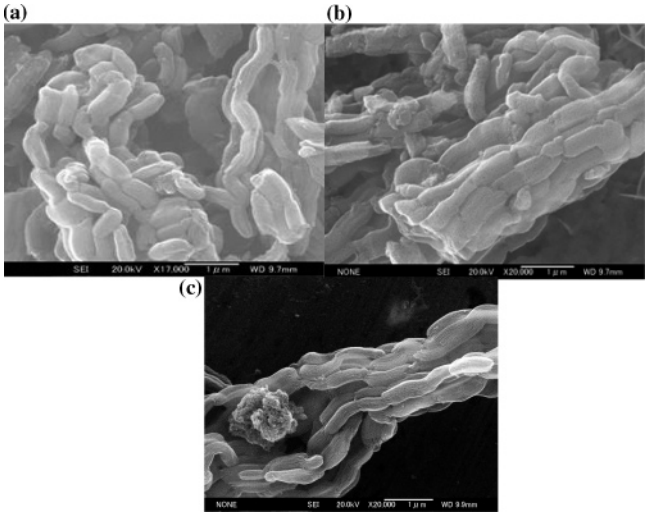

Figure 4. High-resolution scanning electron microscopic images of (A) mesoporous carbon, (B) MBCN(1450), and (C) MBN.

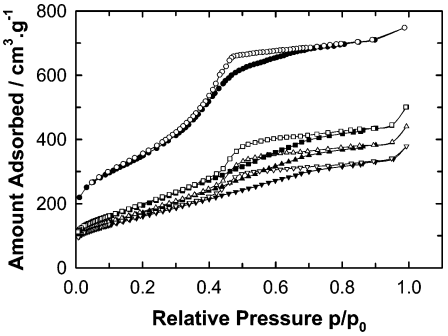

Figure 5. Nitrogen adsorption isotherms of mesoporous carbon, MBCN, and MBN materials: (○, ●) CMK-3, (□, ■) MBCN(1450), (△, ▲) MBCN-(1550), and (▽, ▼) MBN (open symbols: adsorption; closed symbols: desorption).

Information on the textural properties of porous solids are typically obtained from low-temperature (−196 °C) nitrogen adsorption isotherms, which allow the determination of the specific surface area, specific pore volume, and mesopore size distribution. Figure 5 displays the nitrogen adsorption−desorption isotherms of the mesoporous carbon, MBN, MBCN(1450), and MBCN(1550). The nitrogen adsorption isotherms of all the samples are found to be of type IV (as per the IUPAC classification) and exhibit a H1 type broad hysteresis loop, which is typical of mesoporous solids. As the relative pressure increases ($p/p_0 > 0.4$), all isotherms exhibit a sharp step characteristic of capillary condensation of nitrogen within uniform mesopores, where the p/p_0 position of the inflection point is correlated to the diameter of the mesopore. For mesoporous carbon, the adsorption branch of the isotherm shows the point of inflection at relative pressure value of about 0.35. By contrast, a point of reflection at a relative pressure of about 0.45 is noticed for MBN and MBCN samples. The steepness of the capillary condensation steps observed at high relative pressure in MBN and MBCN clearly indicates that they are highly mesoporous and have narrow pore size distribution.

The estimated textural parameters such as specific surface area, specific pore volume, and pore diameter for all the samples are compiled in Table 1. The surface area and pore volume of the MBN and MBCN materials are much lower

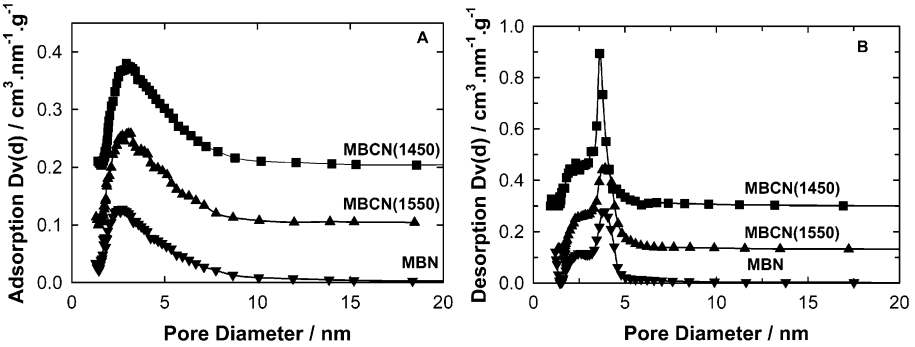

Figure 6. BJH pore size distribution of MBN and MBCN materials: (A) adsorption pore size distribution and (B) desorption pore size distribution.

Table 1. Textural Parameters of Mesoporous Carbon, BN, and BCN Materials

material	A_{BET} (m^2/g)	V_p (cm^3/g)	adsorption, $d_{p,BJH}$ (nm)
mesoporous carbon	1260	1.1	3.0
MBCN(1450)	740	0.69	3.1
MBCN(1550)	650	0.60	3.1
MBN	565	0.53	2.7

as compared to the mesoporous carbon template. This is mainly attributed to the partial pore structural collapse experienced during the substitution reaction at high temperature.

It can also be seen from the Table 1 that the BET surface area, mesopore volume, and pore diameter decrease with decreasing the carbon content in the MBCN samples. MBCN(1450) and MBCN(1550) materials possess relatively high surface areas of 740 and 650 m^2/g and large pore volumes of 0.69 and 0.60 cm^3/g, respectively. However, the specific surface area and the specific pore volume of MBN are 565 m^2/g and 0.53 cm^3/g, respectively, which are much higher as compared to activated BN (168 m^2/g), which was recently reported by Han et al.[33] The pore size distributions (PSD), calculated from the adsorption branch of the nitrogen adsorption−desorption isotherm of MBN and MBCN samples, using BJH method are shown in Figure 6A. The adsorption PSD of all samples is uniform but slightly broader than the PSD of parent mesoporous carbon template.[16,19] On the other hand, the BJH desorption PSD gives a bimodal distribution with the characteristic pore sizes of 2.5 and 4.0 nm in the MBN and MBCN samples (Figure 6B). The large difference in the PSD calculated from the adsorption and desorption branches indicates that the pore structure of MBN and MBCN samples is not homogeneous and they contain an appreciable amount of mesopores of irregular shapes. These pores are responsible for the broad hysteresis loop and delayed capillary evaporation and could lead to pore blocking during the desorption process.

Conclusion

In conclusion, we demonstrated the successful synthesis of mesoporous BN and BCN using mesoporous carbon as a template. These materials possess high specific surface area and specific pore volume. To the best of our knowledge, the synthesis of mesoporous BN and BCN based materials has not been reported hitherto. Furthermore, these porous ceramic structures exhibit a large surface area and pore volume. Thus, we believe that these materials could be used as catalytic supports operating at high temperature in an oxidative atmosphere. They could also be used for the fabrication of batteries and fuel cells because the materials are chemically inert and quite resistant to oxidation. Finally, the synthesis of mesoporous materials using a similar technique could now be extended to the synthesis of other metal nitrides such as GaN, AlN, and Si_3N_4.

Acknowledgment. This study was performed through Special Coordination Funds for Promoting Science and Technology from the Ministry of Education, Culture, Sports, Science and Technology of the Japanese Government. We thank CONACYT-México grants: 41464-Inter American Collaboration (M.T.) and 2004-01-013/SALUD-CONACYT (M.T.).

Supporting Information Available: Two figures showing the XPS survey spectrum of MBN and of MBCN(1450). This material is available free of charge via the Internet at http://pubs.acs.org.

CM051780J